



This is a PDF file of the manuscript  
that has been accepted for publication.  
This file will be reviewed by the authors and editors  
before the paper is published in its final form.  
Please note that during the production process errors  
may be discovered which could affect the content.  
All legal disclaimers that apply to the journal pertain.

## **Ontogenetic changes in the craniomandibular skeleton of the abelisaurid dinosaur *Majungasaurus crenatissimus* from the Late Cretaceous of Madagascar**

NIRINA O. RATSIMBAHOLISON, RYAN N. FELICE, and PATRICK M. O'CONNOR

Ratsimbaholison, N.O., Felice, R.N., and O'Connor, P.M. 2016. Ontogenetic changes in the craniomandibular skeleton of the abelisaurid dinosaur *Majungasaurus crenatissimus* from the Late Cretaceous of Madagascar. *Acta Palaeontologica Polonica* 61 (X): xxx-xxx. <http://dx.doi.org/10.4202/app.00132.2014>

Abelisaurid theropods were one of the most diverse groups of predatory dinosaurs in Gondwana during the Cretaceous Period. The group is characterized by a tall, wide skull and robust cervical region. This morphology is thought to have facilitated specialized feeding behaviors such as prolonged contact with prey. The Late Cretaceous abelisaurid *Majungasaurus crenatissimus* typifies this abelisaurid cranial morphotype. Recent fossil discoveries of this species include a partial growth series that allows for the first time an investigation of ontogenetic variation in cranial morphology in a representative abelisaurid. Herein we examine growth trajectories in the shape of individual cranial bones and articulated skulls of *Majungasaurus* using geometric morphometrics. Several major changes in skull shape were observed through ontogeny, including an increase in the height of the jugal, postorbital, and quadratojugal, an increase in the extent of the contacts between bones, and a decrease in the circumference of the orbit. The skull transitions from relatively short in the smallest individual to tall and robust in large adults, as is seen in other theropods. Such morphological change during ontogeny would likely have resulted in different biomechanical properties and feeding behaviors between small and large individuals. These findings provide a post-hatching developmental framework for understanding the evolution of the distinctive tall skull morphology seen in abelisaurids and other large-sized theropod dinosaurs.

Key words: Abelisauridae, nonavian theropod, geometric morphometrics, ontogeny, skull, Cretaceous, Gondwana.

*Nirina O. Ratsimbaholison [ratsimbano@gmail.com], Department of Paleontology and Biological Anthropology, University of Antananarivo, BP 906, Antananarivo 101, Madagascar; Ohio Center for Ecology and Evolutionary Studies, 228 Irvine Hall, Athens, Ohio 45701 USA.*

*Ryan N. Felice [ryanfelice@gmail.com], Ohio Center for Ecology and Evolutionary Studies, 228 Irvine Hall, Athens, Ohio 45701 USA; Department of Biological Sciences, Ohio University, 228 Irvine Hall, Athens, Ohio 45701, USA; current address: Department of Genetics, Evolution and Environment, University College London, London, UK.*

*Patrick M. O'Connor [oconnorp@ohio.edu] (corresponding author), Ohio Center for Ecology and Evolutionary Studies, 228 Irvine Hall, Athens, Ohio 45701 USA; Department of Biomedical Sciences, Ohio University Heritage College of Osteopathic Medicine, 228 Irvine Hall, Athens, Ohio 45701, USA.*

Received 14 October 2014, accepted 20 January 2016, available online 17 February 2016.

Copyright © 2016 N.O. Ratsimbaholison et al. This is an open-access article distributed under the terms of the Creative Commons Attribution License (for details please see <http://creativecommons.org/licenses/by/4.0/>), which permits unrestricted use, distribution, and reproduction in any medium, provided the original author and source are credited.

## Introduction

It is well appreciated that Tyrannosauridae occupied the large-predator niche in the Northern Hemisphere during the Late Cretaceous Period. By contrast, abelisaurids were among the most diverse nonavian theropod dinosaurs on Gondwanan landmasses during this same interval.

Abelisaurids are considered members of Ceratosauria (Carrano and Sampson 2008), a diverse lineage of Jurassic through Cretaceous theropod dinosaurs that exhibit a vast array of body sizes and morphologies (Gilmore 1920; Madsen and Welles 2000; Xu et al. 2009; Carrano et al. 2011; Pol and Rauhut 2012; Novas et al. 2013), and they occupy distinct regions of cranial morphospace (Brusatte et al. 2012; Foth and Rauhut 2013a). Abelisauridae is best represented during the middle and Late Cretaceous from different regions of the former southern supercontinent of Gondwana, including South America (*Abelisaurus comahuensis*, Bonaparte and Novas 1985; *Carnotaurus sastrei*, Bonaparte et al. 1990; *Ilokelesia aguadagrandensis*, Coria and Salgado 1998; *Aucasaurus garridoi*, Coria et al. 2002; *Ekrixinatosaurus novasi*, Calvo et al. 2004; *Skorpiovenator bustingorryi*, Canale et al. 2008), India (*Indosaurus matleyi*, Huene and Matley 1933; Novas et al. 2004; *Rajasaurus narmadensis*, Wilson et al. 2003), Madagascar (*Majungasaurus crenatissimus*, Depéret 1896a, b; Sampson et al. 1998; Sampson and Witmer 2007; *Dahalokely tokana*, Farke and Sertich 2013), continental Africa (*Rugops primus*, Sereno et al. 2004; *Kryptops palaios*, Sereno and Brusatte 2008) and adjacent areas (e.g., southern Europe; *Genusaurus sisteronis*, Accarie et al. 1995). These discoveries have provided a glimpse of regional diversity and variability within the clade (Carrano and Sampson 2008; Novas et al. 2013; Méndez 2014).

Among the best known of the abelisaurids is *Majungasaurus crenatissimus* from the Late Cretaceous Maevarano Formation exposed in northwestern Madagascar (Sampson and Krause

2007). The skull of this taxon was thoroughly described (Sampson and Witmer 2007) on the basis of well-preserved materials; this taxon typifies the characteristic tall, rostrocaudally short and dorsoventrally tall skull of Abelisauridae. Several additional skulls and partial skeletons have since been recovered that represent multiple, size-diverse specimens (O'Connor et al. 2011; Burch and Carrano 2012). As such, *Majungasaurus* (Fig. 1) has emerged as one of the best-documented species of nonavian theropod dinosaurs from Gondwana, allowing for the first time the formulation of questions related to characterizing intraspecific and ontogenetic variation in Abelisauridae.

Geometric morphometric approaches are commonly used to quantify and visualize interspecific or intraspecific shape variation across a number of specimens or species (e.g., Rohlf and Marcus 1993; Adams et al. 2004, 2013; Zelditch et al. 2004). These approaches have been used to examine topics ranging from assessing basic shape variation (Breuker et al. 2006; Piras et al. 2011; Openshaw and Keogh 2014), justifying species assignments (Baltanás and Danielopol 2011; De Meulemeester et al. 2012), developing biomechanical models (Sakamoto 2010), and testing macroevolutionary hypotheses (e.g., resource partitioning; Kassam et al. 2003).

Morphometric studies have also been used in many paleontological applications, ranging from studies aimed at understanding the locomotor potential in now-extinct clades (Bonnar 2007) to characterizing tempo and mode of cranial evolution (Meloro and Jones 2012), with many recent examples from invertebrate (e.g., Baltanás and Danielopol 2011; Webster and Zelditch 2011) and vertebrate (e.g., Chapman 1990; Stayton and Ruta 2006; Schott et al. 2011; Martin-Serra et al. 2014) groups. Geometric morphometric studies have less frequently focused on dinosaurs, although a recent interest in applying these approaches to the group has resulted in a number of studies (e.g., Young and Larvan 2010; Campione and Evans 2011, Foth and Rauhut

2013a, b; Hedrick and Dodson 2013; Mairino et al. 2013). Several efforts have examined the skull of nonavian theropod dinosaurs, quantifying aspects of craniofacial variability such as cranial diversity and shape disparity, modeling function among different cranial morphs, and hypothesizing putative evolutionary processes producing shape variability in the clade (Young et al. 2010; Zanno and Makovicky 2011; Bhullar et al. 2012; Brusatte et al. 2012; Foth 2013; Foth and Rauhut 2013a). For example, Carpenter (1990) found (qualitatively) that individual variation for *Tyrannosaurus rex* is present in the maxilla, with it exhibiting variability in depth and in the size and shape of the lacrimal and jugal processes. More recent, quantitative research on larger-scale (macroevolutionary) issues across Theropoda indicates that cranial anatomy in this clade is quite variable, with major differences seen in anteroposterior length and snout depth, and to a lesser extent, in orbit size and depth of the cheek region (Brusatte et al. 2012; Foth and Rauhut 2013a). These studies have shown that snout shape and length of the postorbital region ultimately position theropods into different regions of cranial morphospace. Although we have a relatively thorough understanding of alpha taxonomy, phylogenetics, and basic aspects of cranial shape disparity, there have been relatively few descriptions of ontogenetic changes in the skull of theropod dinosaurs (although see Carr 1999; Carr and Williamson 2004; Rauhut and Fechner 2005; Bever and Norell 2009; Tsuihiji et al. 2011; Bhullar et al. 2012; Canale et al. 2015; Foth et al. 2016).

Previous morphometric work has focused on theropods such as *Allosaurus* and *Tyrannosaurus* (Chapman 1990), with only limited work specifically focused on ceratosaurians (e.g., *Carnotaurus* and *Ceratosaurus*; Mazzetta et al. 1998). One study that did include information from abelisaurids investigated the interspecific cranial shape variation in 35 species of non-avian theropods and basal birds (Foth and Rauhut 2013a). Skull shape in abelisaurids was

found to differ greatly from those of other large bodied predators, being characterized by an unusually deep and short skull (see also Brusatte et al. 2012; Foth et al. 2016). Building on this general context, this study focuses on characterizing changes in skull shape in a growth series in an exemplar abelisaurid. The specific aim of this morphometric analysis is to examine ontogenetic changes in the skull of *Majungasaurus crenatissimus*, using both individual bones and whole/partial skulls, in order to understand the post-hatching development of the characteristic tall and wide abelisaurid skull morphotype.

*Institutional abbreviations.*—FMNH PR, Field Museum of Natural History, Chicago, IL, USA; UA, Université d'Antananarivo, Madagascar.

## Material and methods

The fossils currently assigned to *Majungasaurus crenatissimus* easily represent the most numerous for any abelisaurid (Krause et al. 2007; O'Connor et al. 2011), consisting of at least eight partial skulls and skeletons. In this project we compared skulls that shared at least four bones that span the rostral, middle, and caudal regions of the cranium to characterize the skull as a coherent structure. Tables 1 and 2 provide a list of specimens used in the current study.

In order to interpret ontogenetic shape change in individual cranial bones, we used a combination of 2D and 3D landmark-based geometric morphometric techniques (Fig. 2). For seven bones (premaxilla, maxilla, lacrimal, postorbital, jugal, dentary, and surangular), 2D landmarks and semilandmarks were used. For the quadrate, 3D landmarks and semilandmarks were used to summarize its shape. Point landmarks and semilandmarks were assigned using either tpsDig v2.17 (2D; Rohlf 2013) or Landmark (3D; Wiley et al. 2005), with the coordinate

data analyzed using the Geomorph package in R (Adams and Otárola-Castillo 2013). A list containing an anatomical description of the position of each landmark is provided in Supplemental Table 1. In both approaches all landmarks are Type 2 landmarks (i.e., landmarks that exhibit evidence for geometric homology, such as points of maximal curvature or extremities) in the terminology of Bookstein (1991). Following landmark digitization, identical analytical methods were used for both 2D and 3D data sets. Landmark configurations were subjected to a Generalized Procrustes Alignment (GPA), removing the effects of size, rotation, and position. We also calculated centroid size of each landmark configuration and we used centroid size to determine the smallest and largest specimens for each bone. In addition, the surface texture (e.g., the relative development of surface rugosity; Carr 1999; Canale et al. 2015) was also noted as another proxy of relative skeletal maturity. For the seven 2D data sets, we illustrated shape change through ontogeny by generating deformation grids (geometric meshes) demonstrating how these smallest and largest shapes differ from the mean shape (Fig. 2E). These deformation grids were used to aid in interpretation of ontogenetic shape change. For the 3D data set, shape change through ontogeny was illustrated by “warping” a 3D volume of the smallest specimen to fit the landmark configuration of the largest specimen using thin-plate spline interpolation (Fig. 2F; Wiley et al. 2005). Although cranial material of *Majungasaurus crenatissimus* is remarkably well represented, the available sample size is not high enough to facilitate a statistical analysis of ontogenetic shape change. For this reason, we used these GMM geometric morphometric methods to provide a qualitative assessment of ontogenetic shape change rather than to conduct a quantitative analysis.

## Results

Examined individually, each cranial bone shows ontogenetic shape change. The major change in premaxilla morphology is a decrease in the angle between the nasal process and the dorsal margin of the body of the premaxilla and a relative increase in length of the nasal process. This is most marked when comparing FMNH PR 3369 and FMNH PR 2278 (Fig. 3). Shape change in the maxilla was analyzed with landmarks and semilandmarks placed around the perimeter of the maxillary body as incomplete preservation of the ascending ramus makes designating homologous landmarks in the vertical part of this bone impossible. The principal changes in maxilla morphology relate to an increase in height of the rostral part of the maxillary body and a decrease in the degree of sinuosity along the ventral margin. This is best observed by comparing UA 9944 and FMNH PR 2278 (Fig. 4). From a qualitative point of view, the external rugosity (or texturing) on the lateral surface of the maxilla increases with size, as with the other dermal bones of the skull.

Some of the most notable ontogenetic changes in morphology were seen in the bones that surround the orbital and temporal regions of the skull. Although only two lacrimals were available for the analysis, it is apparent that there are major changes in both the overall geometry of the bone and its constituent subparts that influence adjacent craniofacial features (e.g., size of the orbit) from small to large forms (Fig. 5). Specifically, there is a relative decrease in the dorsoventral height of the whole bone, a general increase in size of the lacrimal body, and a decrease in the circumference of the orbital margin formed by the lacrimal. The decrease results from both deposition of bone around the orbital margin of the lacrimal and an increase in relative size of the sub-orbital process. Also, the morphology of the rostral ramus changes substantially, where it extends rostrally in the small form, but is significantly curved rostroventrally (equally



rostral and ventral) in the large form (Fig. 5). Given the limited sample size, the incorporation of additional lacrimals is essential to distinguish whether this latter feature is indeed size related, or rather, if it pertains to intraspecific variability.

Three postorbitals were compared in this analysis, where the dorsal margin is relatively rostrocaudally short in the large mature bones. There is also narrowing of the orbital margin (i.e., the part of the postorbital that is closest to the lateral aperture of the orbit; Fig. 6), similar to that observed above for the lacrimal. Three jugals were compared in the study, where there is a relative increase in dorsoventral height of the lacrimal process and a generalized relative increase in the rostrocaudal length of the bone expressed in the rostral part of the bone, the base of the suborbital process, and the caudal part of the bone (i.e., at the quadratojugal process). These changes coincide with an increase in the dorsoventral height of the articulation between the quadratojugal and jugal (Fig. 7). Notable differences in the quadrate shape across the growth series include a relative decrease in the caudally-directed concavity and an increase in height of the dorsal half of the quadrate shaft (Fig. 8; also see videos at SOM 3 and 4, available at [http://app.pan.pl/SOM/app61-Ratsimbaholison\\_etal\\_SOM.pdf](http://app.pan.pl/SOM/app61-Ratsimbaholison_etal_SOM.pdf)). Although the quadrate was examined in 3D, the major differences through the growth series are best appreciated in lateral view. Mandibular bones variably exhibit ontogenetic shape change as well. A series of three dentaries show major changes including a relative increase in overall height and a change from angular to rounded rostroventral corner convexity (Fig. 9). Three surangulars were included in the analysis, with little noticeable differences apparent over the size range examined (Fig. 10).

Three partial associated or articulated skulls of *Majungasaurus crenatissimus*, ranging in estimated length from 42 cm to 53 cm (SOM 2), were included in a multi-element analysis. The use of these specimens served to identify any skull characteristics related to changes in the nature

of articulations among elements over the growth series. Despite the fact that *Majungasaurus* is known from many specimens of diverse ontogenetic (size) classes and represents a good candidate for ontogenetic research, many of the partial skulls provide limited information for the current study. Specifically, nonoverlapping preservation of bones (Fig. 1A–C) renders the dataset useful for characterizing selected regions (e.g., postorbital region), whereas it limits potential information from other regions (e.g., rostradorsal narial region). In sum, 17 landmarks and 16 semilandmarks were compared for these three skulls in a 2D, lateral view perspective (Fig. 1).

Examination of the skull shape deformation grids reveals several growth changes in the skull. First, there is a relative increase in dorsoventral height of the lacrimal process of the jugal and rostrocaudal length of the rostral part of the jugal. These changes coincide with an increase in the dorsoventral height of the articulation between the quadratojugal and jugal. The orientation of the jugal is rotated in larger individuals such that the contact between the jugal and maxilla is positioned relatively more dorsal than the jugal-quadratojugal contact. Second, the orbit becomes smaller relative to the size of the skull. For example, the ventral portion of the orbit becomes taller and rostrocaudally shorter. This corresponds to a shortening of the jugal process of the quadratojugal. The caudal margin of the dorsal region of the orbit (i.e., the orbit proper) decreases in diameter. Finally, the temporal region of the skull increases in height due to the relative increase in height between the squamosal process of postorbital and quadrate process of quadratojugal, which changes the inclination of the jugal (Fig. 1).

## Discussion

This study has resulted in a number of observations related to craniomandibular skeletal ontogeny in *Majungasaurus crenatissimus*. These changes may be consistent with patterns in

abelisaurids in general given the shared possession of tall, short skulls in the clade. The fossil record of *Majungasaurus crenatissimus* is notable (n = 8 partial/whole skulls) among Abelisauridae, but is still too limited to allow for rigorous statistical evaluation of shape change (e.g., significance of allometric shape change). Nonetheless, our results provide important observations for refining primary hypotheses regarding skull shape change through ontogeny in the group.

**Ontogenetic shape change in individual elements.**—Differential growth in portions of numerous skull bones (e.g., maxilla, quadrate) contribute to the tall skull of larger specimens of *Majungasaurus crenatissimus*. Throughout ontogeny, these elements undergo dorsoventral expansion, as seen in the comparison plots of individual elements (e.g., Figs. 3–9). Taken together, it is apparent that individual skull elements or even component parts of them contribute to the overall adult morphotype seen in *Majungasaurus* (i.e., high skull).

**Ontogenetic shape change of the skull.**—Analysis of the articulated skull is also consistent with ontogenetic dorsoventral expansion. Importantly, only certain regions (e.g., the rostral-most maxilla) of bones making up the rostrum increase in dorsoventral height, whereas the caudal portion of the maxilla is not expanded to the same degree. In contrast, the entire quadrate contributes to increase in dorsoventral height of the skull. This is best exemplified in the increase in height between the squamosal process of the postorbital and the quadrate process of the quadratojugal (Fig. 10). In addition, the orientation of the long axis of the body of the jugal shifts from being relatively horizontal to having a caudoventral-to-rostrrodorsal orientation in larger

specimens. Such changes in orientation through ontogeny contribute to the characteristic tall skull of *Majungasaurus* and abelisaurids more generally.

**Other observations related to ontogenetic changes in *Majungasaurus*.**—Both individual element (e.g., postorbital) and whole skull analyses show changes to the orbit. For example, orbital circumference decreases due to closing of the arc formed along the orbital margin on both the lacrimal and postorbital (Figs. 5, 6). A similar ontogenetic change in orbit shape is seen in other theropods (e.g., Henderson 2002; Foth and Rauhut 2013a; see below). There also appears to be increased connectivity (e.g., sutural rigidity) between bones and changes in the general surface texture of the skull. It is apparent that sutures between adjacent bones become increasingly interlocked during growth. This is best illustrated by the sutural connection between the quadratojugal and jugal, and between the jugal and maxilla (Fig. 1). There is an increase the rugose sculpturing on the external surfaces of many of the skull elements in *Majungasaurus*. Rugose external bone texture has been described as one of the hallmark abelisaurid features (e.g., Sampson and Witmer 2007; Hieronymus 2009; also, see Canale et al. 2015 for additional discussion of this feature in other nonavian theropods). The increasing sculpturing/rugosity of the external surfaced is so pronounced in the larger individuals that it obscures sutural boundaries (e.g., between the postorbital and lacrimal; Fig. 1).

**Intraspecific variation.**—Although the current study sought to examine shape changes in individual elements and whole/partial skulls of *Majungasaurus crenatissimus* as a representative abelisaurid, results from this work also point out significant intraspecific variability that is either completely independent of size-related changes or not directly linked with changes in

growth/size. For example, a decrease in the degree of sinuosity along the ventral margin of the maxilla is apparent through the series (Fig. 4). Moreover, even a simple qualitative assessment of maxilla morphology indicates differences related to the lateral exposure of the antorbital fenestra. Specifically, a comparison of two, similar-sized maxillae reveal one specimen (UA 9944) in which the lateral antorbital fossa (sensu Hendrickx and Mateus 2014) is well exposed, with the other specimen (FMNH PR 3369) exhibiting a virtually nonexistent lateral exposure of the antorbital fossa along the jugal ramus (Fig. 4B, C). It is important to note that such differences existing within a single taxon could have significant implications for assessing the taxonomic uniqueness (i.e., putative autapomorphies) of isolated discoveries (e.g., Russell 1996; Lamanna et al. 2002) or remains that preserve rather limited anatomical information.

**Biomechanical implications of ontogenetic skull change.**—The disproportionate dorsoventral increase in height of the adductor region of the skull implies that adductor muscle length would have had a similar allometric relationships through ontogeny. It is unclear how this might affect bite force production, as there is little constraint on general muscle architecture (e.g., pennate or not) or specific architectural parameters (e.g., degree of pennation) for specific jaw adductors (Holliday 2009; Sakamoto 2010). Importantly, work on other theropods (e.g., Foth and Rauhut 2013a) and extant crocodylians (e.g., Pierce et al. 2008; Foth et al. 2013) has also found shape change differences between the rostral and caudal (i.e., posterior) ends of the skull, suggesting the former relates more to dietary preference (e.g., prey type) and the latter to general allometric considerations related to maintenance of function at larger sizes (e.g., the necessity of producing higher bite forces) and feeding behavior more generally. As such, the observed increase in height of the adductor region in *Majungasaurus* is consistent in this context, particularly when

considering its typical "carnivorous" theropod morphology in dentigerous elements (Foth and Rauhut 2013a). The ontogeny of bite-force generation is positively allometric (e.g., Erickson et al. 2003; also see Erickson et al. 2012 for a more general discussion of the allometry of bite force production in a comparative context). It should also be appreciated, however, that general increases in fiber length (inferred on the basis of positive ontogenetic allometry of the adductor chamber) contribute to both a wider gape and an increased range over which bite forces may be applied to substrates (Herring and Herring 1974, Lautenschlager 2015). Thus, the significance of the observed ontogenetic changes in adductor chamber morphology for feeding mechanics in abelisaurids remains to be clarified, particularly given that the feeding mechanics in *Majungasaurus* (and other abelisaurids) have only been superficially addressed (e.g., jaw adduction vs. jaw adduction combined with pulling; O'Connor 2007; Sampson and Witmer 2007; Méndez 2014).

**Comparative ontogeny of the nonavian theropod skull.**—The ontogenetic changes in skull shape seen in *Majungasaurus* differ from the patterns typically seen among nonavian theropod dinosaurs. Most non-eumaniraptoran theropods (e.g., *Coelophysis*, Compsognathidae) increase the length of the face and decrease the height of the lower temporal fenestra through ontogeny, resulting in a more slender skull in adults than in juveniles (Bhullar et al. 2012). The opposite is seen in *Majungasaurus*, which has a taller skull and temporal region in adults than juveniles. However, this trend compares favorably to patterns in so-called “giant theropods” of various clades, including ceratosaurs, allosauroids, and tyrannosauroids (Bhullar et al. 2012). The giant taxa exhibit a novel developmental trajectory that is similar to the “typical” theropod condition (i.e., rostrocaudal elongation), but this changes to an increase of the dorsoventral dimension of

the skull (Bhullar et al. 2012), resulting in a tall skull. This ontogenetic pattern is hypothesized to have evolved convergently in all large-bodied theropods (Bhullar et al. 2012) and is likely to be an example of peramorphic heterochrony (Canale et al. 2015). As the skull of *Majungasaurus* also increases in height through ontogeny, it is possible that it shares the developmental trajectory of other large-bodied theropods. Additional perinatal or very small juvenile specimens are needed to determine whether *Majungasaurus* transitions through an initial phase of elongation before increasing in height, similar to the pattern observed in *Tyrannosaurus* and other large-sized theropods.

## Conclusions

The ontogenetic skull changes of *Majungasaurus crenatissimus* include (i) increase in skull height, (ii) increased sutural interlocking between cranial elements, and (iii) increased surface texturing on certain elements (e.g., maxilla) as size increases. The overall shape differences in the growth series are achieved through shape changes in individual elements including the quadrate, postorbital, lacrimal and jugal, in addition to differential growth in some sub-regions of individual elements (e.g., the rostral part of the maxilla). This effort characterizes craniomandibular ontogeny in an exemplar abelisaurid, one necessary step for understanding the extensive radiation of the group throughout Gondwanan and better placing it in an ecological setting.

## Acknowledgements

A very special thanks to Joseph Groenke (Stony Brook University, USA) for the preparation, molding, casting, and CT-scanning of all previously-unpublished *Majungasaurus* specimens

used in this study. We also thank David Krause (Stony Brook University, USA), Joseph Sertich (Denver Museum of Science and Nature, USA), Eric Lund and Waymon Holloway (both Ohio University, Athens, USA), and other members of the Mahajanga Basin Project for advice and logistical support during the development and execution of this project. Haingoson Andriamialison and Armand Rasoamiaramanana (Department of Paleontology and Biological Anthropology, University of Antananarivo, Madagascar) are thanked for their support. Susan Williams (Ohio University, Athens, USA), Casey Holliday (University of Missouri, Columbia, USA), and Lawrence Witmer (Ohio University, Athens, USA) provided useful discussions. Christian Foth and Thomas Carr are thanked for providing comments on an earlier version of this manuscript. This work was supported by the National Science Foundation (EAR-0446488, EAR-0617561, and EAR-1123642), the Ohio University Office of Research and Sponsored Programs, the Ohio University Heritage College of Osteopathic Medicine, and SVP SEDN-Program for Scientists from Economically Developing Nations.

## References

- Accarie, H., Beaudoin, B., Dejax, J., Fries, G., Micard, J.-G., and Taquet, P. 1995. Découverte d'un dinosaure théropode nouveau (*Genusaurus sisteronis* n. g., n. sp.) dans l'Albien marin de Sisteron (Alpes de Haute-Provence, France) et extension au Crétacé inférieur de la lignée cératosaurienne. *Comptes Rendus de l'Académie Sciences, Paris, Série IIa* 320: 327–334.
- Adams, D.C. and Otárola-Castillo, E. 2013. geomorph: an R package for the collection and analysis of geometric morphometric shape data. *Methods in Ecology and Evolution* 4: 393–399. <http://dx.doi.org/10.1111/2041-210X.12035>
- Adams, D., Rohlf, F., and Slice, D. 2004. Geometric morphometrics: ten years of progress following the 'revolution'. *Italian Journal of Zoology* 71: 5–16. <http://dx.doi.org/10.1080/11250000409356545>
- Adams, D.C., Rohlf, F.J., and Slice, D.E. 2013. A field comes of age: geometric morphometrics in the 21st century. *Hystrix, Italian Journal of Mammalogy* 24: 7–14.



- Baltanás, A. and Danielopol, D.L. 2011. Geometric Morphometrics and its use in ostracod research: a short guide. *Joannea Geologie und Paläontologie* 11: 235–272.
- Bever, G.S. and Norell, M. 2009. The perinate skull of *Byronosaurus* (Troodontidae) with observations on the cranial ontogeny of paravian theropods. *American Museum Novitates* 3657: 1–51. <http://dx.doi.org/10.1206/650.1>
- Bhullar, B.A., Marugan-Lobon, J., Racino, F., Bever, G.S., Rowe, T.B., Norell, M.A., and Abzhanov, A. 2012. Birds have paedomorphic dinosaur skulls. *Nature* 487: 223–226. <http://dx.doi.org/10.1038/nature11146>
- Bonaparte, J.F. and Novas, F.E. 1985. *Abelisaurus comahuensis* new carnosauria from Late Cretaceous of Patagonia. *Ameghiniana* 21: 259–265.
- Bonaparte, J.F., Novas, F.E., and Coria, R. 1990. *Carnotaurus sastrei* Bonaparte, the horned, lightly built carnosaur from the middle Cretaceous of Patagonia. *Natural History Museum of Los Angeles County, Contributions in Science* 416: 1–41.
- Bonnan, M.F. 2007. Linear and geometric morphometric analysis of long bone scaling patterns in Jurassic neosauropod dinosaurs: their functional and paleobiological implications. *Anatomical Record* 290: 1089–1111. <http://dx.doi.org/10.1002/ar.20578>
- Bookstein, F.L. 1991. *Morphometric Tools for Landmark Data*. 456 pp. Cambridge University Press, Cambridge.
- Breuker, C.J., Patterson, J.S., and Klingenberg, C.P. 2006. A single basis for developmental buffering of *Drosophila* wing shape. *PLoS ONE* 1: e7. <http://dx.doi.org/10.1371/journal.pone.0000007>
- Brusatte, S.L., Sakamoto, M, Montanari, S., and Smith, W.E.H. 2012. The evolution of cranial form and function in theropod dinosaurs: insights from geometric morphometrics. *Journal of Evolutionary Biology* 25: 365–377. <http://dx.doi.org/10.1111/j.1420-9101.2011.02427.x>
- Burch, S.H., and Carrano, M.T. 2012. An articulated pectoral girdle and forelimb of the abelisaurid theropod *Majungasaurus crenatissimus* from the Late Cretaceous of Madagascar. *Journal of Vertebrate Paleontology* 32: 1–16. <http://dx.doi.org/10.1080/02724634.2012.622027>
- Canale, J.I., Novas, F.E., Salgado, L., and Coria, R.A. 2015. Cranial ontogenetic variation in *Mapusaurus roseae* (Dinosauria: Theropoda) and the probable role of heterochrony in carcharodontosaurid evolution. *Paläontologische Zeitschrift* 89: 983–993. <http://dx.doi.org/10.1007/s12542-014-0251-3>

Canale, J.I., Scanferla, C.A., Agnolin, F.L., and Novas, F.E. 2008. New carnivorous dinosaur from the Late Cretaceous of NW Patagonia and the evolution of abelisaurid theropods. *Naturwissenschaften* 96: 409–414. <http://dx.doi.org/10.1007/s00114-008-0487-4>

Calvo, J.O., Rogers-Rubilar, D., and Moreno, K. 2004. A new Abelisauridae (Dinosauria: Theropoda) from northwest Patagonia. *Ameghiniana* 41: 555–563.

Campione, N.E. and Evans, D.C. 2011. Cranial growth and variation in edmontosaurs (Dinosauria: Hadrosauridae): implications for latest Cretaceous megaherbivore diversity in North America. *PLoS ONE* 6 (9): e25186. <http://dx.doi.org/10.1371/journal.pone.0025186>

Carpenter, K. 1990. Variation in *Tyrannosaurus rex*. In: K. Carpenter and P.J. Currie (eds.), *Dinosaur Systematics: Perspectives and Approaches*, 141–145. Cambridge University Press, Cambridge. <http://dx.doi.org/10.1017/cbo9780511608377.013>

Carr, T.D. 1999. Craniofacial ontogeny in Tyrannosauridae (Dinosauria, Coelurosauria). *Journal of Vertebrate Paleontology* 19: 497–520. <http://dx.doi.org/10.1080/02724634.1999.10011161>

Carr, T.D. and Williamson, T.E. 2004. Diversity of late Maastrichtian Tyrannosauridae (Dinosauria: Theropoda) from western North America. *Zoological Journal of the Linnean Society* 142 (4): 479–523. <http://dx.doi.org/10.1111/j.1096-3642.2004.00130.x>

Carrano, M.T. and Sampson, S.D. 2008. The Phylogeny of Ceratosauria (Dinosauria: Theropoda). *Journal of Systematic Palaeontology* 6: 183–236. <http://dx.doi.org/10.1017/S1477201907002246>

Carrano, M.T., Loewen, M.A., and Sertich, J.J.W. 2011. New materials of *Masiakasaurus knopfleri* Sampson, Carrano, and Forster, 2001, and implications for the morphology of the Noosauridae (Theropoda: Ceratosauria). *Smithsonian Contribution to Paleobiology* 95: 1–53. <http://dx.doi.org/10.5479/si.00810266.95.1>

Chapman, R.E. 1990. Shape analysis in the study of dinosaur morphology. In: K. Carpenter and P.J. Currie (eds.), *Dinosaur Systematics: Approaches and Perspectives*, 21–42. Cambridge University Press, Cambridge. <http://dx.doi.org/10.1017/cbo9780511608377.005>

Coria, R.A. and Salgado, L. 1998. A basal Abelisauria Novas, 1992 (Theropoda-Ceratosauria) from the Cretaceous of Patagonia, Argentina. *Gaia* 15: 89–102.

Coria, R.A., Chiappe, L.M., and Dingus, L. 2002. A new close relative of *Carnotaurus sastrei* Bonaparte 198 (Theropoda: Abelisauridae) from the Late Cretaceous of Patagonia. *Journal of Vertebrate Paleontology* 22: 460–465. [http://dx.doi.org/10.1671/0272-4634\(2002\)022\[0460:ANCROC\]2.0.CO;2](http://dx.doi.org/10.1671/0272-4634(2002)022[0460:ANCROC]2.0.CO;2)

De Meulemeester, T., Michez, D., Aytekin, A.M., and Danforth, B.N. 2012. Taxonomic affinity of halictid bee fossils (Hymenoptera: Anthophila) based on geometric morphometrics analyses of wing shape. *Journal of Systematic Palaeontology* 10: 755–764.

<http://dx.doi.org/10.1080/14772019.2011.628701>

Depéret, C. 1896a. Note sur les Dinosauriens Sauropodes et Théropodes du Crétacé supérieur de Madagascar. *Bulletin de la Société Géologique de France* 21: 176–194.

Depéret, C. 1896b. Sur l'existence de Dinosauriens, Sauropodes et Théropodes dans le Crétacé supérieur de Madagascar. *Comptes Rendus de l'Académie des Sciences (Paris), Série II* 122: 483–85.

Erickson, G.M., Lappin, A.K., and Vliet, K.A. 2003. The ontogeny of bite-force performance in American alligator (*Alligator mississippiensis*). *Zoological Society of London* 260: 317–327.

<http://dx.doi.org/10.1017/S0952836903003819>

Erickson, G.M., Gignac, P.M., Stepan, S.J., Lappin, A.K., Vliet, K.A., Brueggen, J.D., Inouye, B.D., Kledzik, D., and Webb, G.J.W. 2012. Insights into the ecology and evolutionary success of crocodylians revealed through bite-force and tooth-pressure experimentation. *PLoS ONE* 7: e31781. <http://dx.doi.org/10.1371/journal.pone.0031781>

Farke, A.A. and Sertich, J.J.W. 2013. An Abelisauroid theropod dinosaur from the Turonian of Madagascar. *PLoS ONE* 8: e62047. <http://dx.doi.org/10.1371/journal.pone.0062047>

Foth, C. 2013. Ontogenetic, Macroevolutionary, and Morphofunctional Patterns in Archosaur Skulls: A Morphometric Approach. Unpublished Ph.D. Dissertation. 369 pp. Ludwig Maximilians University, Munich.

Foth, C. and Rauhut, O.W.M. 2013a. Macroevolutionary and morphofunctional patterns in theropod skulls: a morphometric approach. *Acta Palaentologica Polonica* 58: 1–16.

Foth, C., and Rauhut, O.W.M. 2013b. The good, the bad, and the ugly: The influence of skull reconstructions and intraspecific variability in studies of cranial morphometrics in theropods and basal saurischians. *PLoS ONE* 8: e72007.

<http://dx.doi.org/10.1371/journal.pone.0072007>

Foth, C., Bona, P., and Desojo, J.B. 2013. Intraspecific variation in the skull morphology of the black caiman *Melanosuchus niger* (Alligatoridae, Caimaninae). *Acta Zoologica* 96: 1–13.

<http://dx.doi.org/10.1111/azo.12045>

Foth, C., Hedrick, B.P., and Ezcurra, M.D. 2016. Cranial ontogenetic variation in early saurischians and the role of heterochrony in the diversification of predatory dinosaurs. *PeerJ* 4: e1589.

Gilmore, C.W. 1920. Osteology of the carnivorous Dinosauria in the United States National Museum, with special reference to the genera *Antrodemus* (*Allosaurus*) and *Ceratosaurus*. Bulletin of the United States National Museum 110: 1–159.

<http://dx.doi.org/10.5962/bhl.title.61883>

Hedrick, B.P. and Dodson, P. 2013. Lujiatun psittacosaurids: understanding individual and taphonomic variation using 3D geometric morphometrics. PLoS ONE 8: e69265.

<http://dx.doi.org/10.1371/journal.pone.0069265>

Henderson, D.M. 2002. The eyes have it: The sizes, shapes, and orientations of theropod orbits as indicators of skull strength and bite force. Journal of Vertebrate Paleontology 22: 766–778.

[http://dx.doi.org/10.1671/0272-4634\(2002\)022\[0766:TEHITS\]2.0.CO;2](http://dx.doi.org/10.1671/0272-4634(2002)022[0766:TEHITS]2.0.CO;2)

Hendrickx, C. and Mateus, O. 2014. *Torvosaurus gurneyi* n. sp., the largest terrestrial predatory from Europe, and a proposed terminology of the maxilla anatomy in nonavian theropods. PLoS ONE 9: e88905.

<http://dx.doi.org/10.1371/journal.pone.0088905>

Herring, S.W. and Herring, S.E. 1974. The superficial masseter and gape in mammals.

American Naturalist 108: 561–576. <http://dx.doi.org/10.1086/282934>

Hieronymus, T.L. 2009. Osteological Correlates of Cephalic Skin Structures in Amniota: Documenting the Evolution of Display and Feeding Structures with Fossil Data. 254 pp. Unpublished Ph.D. Dissertation, Ohio University, Athens.

Holliday, C.M. 2009. New insights into dinosaur jaw muscle anatomy. Anatomical Record 292:

1246–1265. <http://dx.doi.org/10.1002/ar.20982>

Huene, F. von and Matley, C.A. 1933. The Cretaceous Saurischia and Ornithischia of the Central Provinces of India. Memoirs of the Geological Society of India: Palaeontologica Indica 21: 1–72.

Kassam, D.D., Adams, D.C., Ambali, A., and Yamaoka, K. 2003. Body shape variation in relation to resource partitioning within cichlid trophic guilds coexisting along the rocky shore of Lake Malawi. Animal Biology 53: 59–70. <http://dx.doi.org/10.1163/157075603769682585>

Krause, D.W., Sampson, S.D., Carrano, M.T., and O'Connor, P.M. 2007. Overview of the history of the discovery, taxonomy, phylogeny, and biogeography of *Majungasaurus crenatissimus* (Theropoda: Abelisauridae) from the Late Cretaceous of Madagascar. Journal of Vertebrate Paleontology, Memoir 8: 1–20.

Lamanna, M.C., Martínez, R.D., and Smith, J.B. 2002. A definitive abelisaurid theropod dinosaur from the Early Cretaceous of Patagonia. Journal of Vertebrate Paleontology 22: 58–

69. [http://dx.doi.org/10.1671/0272-4634\(2002\)022\[0058:ADATDF\]2.0.CO;2](http://dx.doi.org/10.1671/0272-4634(2002)022[0058:ADATDF]2.0.CO;2)

Lautenschlager S. 2015. Estimating cranial musculoskeletal constraints in theropod dinosaurs. Royal Society Open Science 2: 150495. <http://dx.doi.org/10.1098/rsos.150495>

Madsen J.H. and Welles, S.P. 2000. *Ceratosaurus* (Dinosauria, Theropoda). A revised osteology. Miscellaneous Publications of the Utah Geological Survey 00-2: 1–80.

Maoirino, L., Farke, A.A, Kotsakis, T., and Piras, P. 2013. Is *Torosaurus* *Triceratops*? Geometric morphometric evidence of Late Maastrichtian Ceratopsid dinosaurs. PLoS ONE 8: e81608. <http://dx.doi.org/10.1371/journal.pone.0081608>

Martin-Serra A., Figuerido, B., and Palmqvist, P. 2014. A three-dimensional analysis of morphological evolution and locomotor performance of the carnivoran forelimb. PLoS ONE 9: 1–20. <http://dx.doi.org/10.1371/journal.pone.0085574>

Mazzetta, G.V., Farina, R.A., and Vizcaino, S.F. 1998. On the palaeobiology of the South American horned theropod *Carnotaurus sastrei* Bonaparte. Gaia 15: 185–192.

Meloro, C.C. and Jones, M.E.H. 2012. Tooth and cranial disparity in the fossil relatives of *Sphenodon* (Rhynchocephalia) dispute the persistent "living fossil" label. Journal of Evolutionary Biology 25: 2194–2209. <http://dx.doi.org/10.1111/j.1420-9101.2012.02595.x>

Méndez, A. 2014. The cervical vertebrae of the Late Cretaceous abelisaurid dinosaur *Carnotaurus sastrei*. Acta Palaeontologica Polonica 59: 569–579.

Novas, F.E., Agnolin, F.L., and Bandyopadhyay S. 2004. Cretaceous theropods from India; a review of specimens described by Huene and Matley (1933). Revista del Museo Argentino de Ciencias Naturales 6: 67–103.

Novas, F.E., Agnolin, F.L., Ezcurra, M.D., Porfiri, J., and Canale, J.I. 2013. Evolution of the carnivorous dinosaurs during the Cretaceous: The evidence from Patagonia. Cretaceous Research 45: 174–215. <http://dx.doi.org/10.1016/j.cretres.2013.04.001>

O'Connor, P.M. 2007. The postcranial axial skeleton of *Majungasaurus crenatissimus* (Theropoda: Abelisauridae) from the Late Cretaceous of Madagascar. Journal of Vertebrate Paleontology, Memoir 8: 127–162.

O'Connor, P.M., Rogers, R.R., Groenke, J.R., Burch, S.H., and Turner, A.H. 2011. A multi-taxon theropod dinosaur accumulation from the Late Cretaceous of Madagascar: near-instantaneous entombment of small-bodied avialans. Journal of Vertebrate Paleontology 31 (Supplement 3): 168.

Openshaw, G.H. and Keogh, J.S. 2014. Head shape evolution in monitor lizards (*Varanus*): interactions between extreme size disparity, phylogeny and ecology. *Journal of Evolutionary Biology* 27: 363–373. <http://dx.doi.org/10.1111/jeb.12299>

Pierce, S.E., Angielczyk, K.D., and Rayfield, E.J. 2008. Patterns of morphospace occupation and mechanical performance in extant crocodylian skulls: a combined geometric morphometric and finite element modeling approach. *Journal of Morphology* 269: 840–864. <http://dx.doi.org/10.1002/jmor.10627>

Piras, P., Salvi, D., Ferrara, G., Maiorino, L., Delfino, M., Pedde, L., and Kotsakis, T. 2011. The role of post-natal ontogeny in the evolution of phenotypic diversity in *Podarcis* lizards. *Journal of Evolutionary Biology* 24: 2705–2720. <http://dx.doi.org/10.1111/j.1420-9101.2011.02396.x>

Pol, D. and Rauhut, O.W.M. 2012. A Middle Jurassic abelisaurid from Patagonia and the early diversification of theropod dinosaurs. *Proceedings of the Royal Society B* 279: 3170–3175. <http://dx.doi.org/10.1098/rspb.2012.0660>

Rauhut, O.W.M. and Fechner, R. 2005. Early development of the facial region in a non-avian theropod dinosaur. *Proceedings of the Royal Society B* 272: 1179–1183. <http://dx.doi.org/10.1098/rspb.2005.3071>

Rohlf, J.F. 2013. tpsDig, Digitize Landmarks and Outlines, version 2.17. Department of Ecology and Evolution, State University of New York, Stony Brook. Available at <http://life.bio.sunysb.edu/morph> (accessed 7/1/2013).

Rohlf, J.F. and Marcus, L.F. 1993. A revolution in morphometrics. *Trends in Ecology and Evolution* 8 (4): 129–132. [http://dx.doi.org/10.1016/0169-5347\(93\)90024-J](http://dx.doi.org/10.1016/0169-5347(93)90024-J)

Russell, D. 1996. Isolated dinosaur bones from the middle Cretaceous of the Tafilalt, Morocco. *Bulletin Muséum National d'Histoire Naturelle, Paris, séries 4C* 18: 349–402.

Sakamoto, M. 2010. Jaw biomechanics and the evolution of biting performance in theropod dinosaurs. *Proceedings of the Royal Society B* 277: 3327–3333. <http://dx.doi.org/10.1098/rspb.2010.0794>

Sampson, S.D. and Krause, D.W. (eds.) 2007. *Majungasaurus crenatissimus* (Theropoda: Abelisauridae) from the Late Cretaceous of Madagascar. *Society of Vertebrate Paleontology Memoir* 8 (Supplement to *Journal of Vertebrate Paleontology* 27 [2]): 1–184.

Sampson, S.D. and Witmer, L.M. 2007. Craniofacial anatomy of *Majungasaurus crenatissimus* (Theropoda: Abelisauridae) from the Late Cretaceous of Madagascar. In: S.D. Sampson and D.W. Krause (eds.), *Majungasaurus crenatissimus* (Theropoda: Abelisauridae) from the Late

Cretaceous of Madagascar. *Society of Vertebrate Paleontology Memoir* 8 (Supplement to *Journal of Vertebrate Paleontology* 27[2]): 32–102.

Sampson, S.D., Witmer, L.M., Forster, C.A., Krause, D.W., O'Connor, P.M., Dodson, P., and Ravoavy, F. 1998. Predatory dinosaur remains from Madagascar: Implications for the Cretaceous biogeography of Gondwana. *Science* 280: 1048–1051.  
<http://dx.doi.org/10.1126/science.280.5366.1048>

Schott, R.K., Evans, D.C., Goodwin, M.B., Horner, J.R., Brown, C.M., and Longrich, N.R. 2011. Cranial ontogeny in *Stegoceras validum* (Dinosauria: Pachycephalosauria): a quantitative model of pachycephalosaur dome growth and variation. *PLoS ONE* 6: e21092.  
<http://dx.doi.org/10.1371/journal.pone.0021092>

Sereno, P.C. and Brusatte, S.L. 2008. Basal abelisaurid and carcharodontosaurid theropods from the Lower Cretaceous Elrhaz Formation of Niger. *Acta Palaeontologica Polonica* 53: 15–46. <http://dx.doi.org/10.4202/app.2008.0102>

Sereno, P.C., Wilson, J.A., and Conrad, J.L. 2004. New dinosaurs link southern landmasses in the Mid-Cretaceous. *Proceedings of the Royal Society B* 271: 1325–1330.  
<http://dx.doi.org/10.1098/rspb.2004.2692>

Stayton, C.T. and Ruta, M. 2006. Geometric morphometrics of the skull roof of stereospondyls (Amphibia: Temnospondyli). *Palaeontology* 49: 307–337.  
<http://dx.doi.org/10.1111/j.1475-4983.2006.00523.x>

Tsuihiji, T., Watabe, M., Tsogtbaatar, K., Tsubamoto, T., Barsbold, R., Suzuki, S., Lee, A. H., Ridgely, R.C., Kawahara, Y., and Witmer, L.M. 2011. Cranial osteology of a juvenile specimens of *Tarbosaurus bataar* (Theropoda, Tyrannosauridae) from the Nemegt Formation (Upper Cretaceous) of Bugin Tsav, Mongolia. *Journal of Vertebrate Paleontology* 31: 497–517.  
<http://dx.doi.org/10.1080/02724634.2011.557116>

Webster, M. and Zelditch, M.L. 2011. Evolutionary lability of integration in Cambrian ptychoparioid trilobites. *Journal of Evolutionary Biology* 38: 144–162.  
<http://dx.doi.org/10.1007/s11692-011-9110-2>

Wiley, D.F., Amenta, N., Alcantara, D.A., Ghosh, D., Kil, Y.J., Delson, E., Harcourt-Smith, W., Rohlf, F.J., John, K.S., and Hamann, B. 2005. Evolutionary morphing. *Proceedings of IEEE visualization 2005*: 431–438.  
<http://dx.doi.org/10.1109/VISUAL.2005.1532826>

Wilson, J.A., Sereno, P.C., and Srivastava, S., Bhatt, D.K., Khosla, A., and Sahni, A. 2003. A new Abelisaurid (Dinosauria, Theropoda) from the Lameta Formation (Cretaceous, Maastrichtian) of India. *Contributions from the Museum of Paleontology, University of Michigan* 31: 1–42.



Xu, X., Clark, J.M., Mo, J., Choiniere, J., Forster, C.A., Erickson, G.M., Hone, D.W.E., Sullivan, C., Eberth, D.A., Nesbitt, S., Zhao, Q., Hernandez, R., Jia, C.-K., Han, F.-L., and Guo, Y. 2009. A Jurassic ceratosaur from China helps clarify avian digital homologies. *Nature* 459: 940–944. <http://dx.doi.org/10.1038/nature08124>

Young, M.T. and Larvan, M.D. 2010. Macroevolutionary trends in the skull of sauropodomorph dinosaurs—the largest terrestrial animals to have ever lived. In: A.M.T. Elewa (ed.), *Morphometrics for Nonmorphometricians. Lecture Notes in Earth Sciences* 124: 259–269.

Young, M.T., Brusatte, S.L., Ruta, M., and De Andrade, M.B. 2010. The evolution of Metriorhynchoidea (Mesoeucrocodylia, Thalattosuchia): an integrated approach using geometric morphometrics, analysis of disparity, and biomechanics. *Zoological Journal of the Linnean Society* 158: 801–859.  
<http://dx.doi.org/10.1111/j.1096-3642.2009.00571.x>

Zanno, L.E. and Makovicky P.J. 2011. Herbivorous ecomorphology and specialization patterns in theropod dinosaur evolution. *Proceedings of the National Academy of Sciences* 108: 232–237. <http://dx.doi.org/10.1073/pnas.1011924108>

Zelditch, M.L., Swiderski, D.L., Sheets, H.D., and Fink, W.L. 2004. *Geometric Morphometrics for Biologists: A Primer*. 443 pp. Elsevier Academic Press, San Diego.



## FIGURE CAPTIONS

Fig. 1. Whole (B) and partial (A) skulls (rendered CT images) of *Majungasaurus crenatissimus* (Depéret, 1896) Lavocat, 1955 from the Maastrichtian (Late Cretaceous) Maevarano Formation, northwestern Madagascar in left lateral view. **A.** UA 9944. **B.** FMNH PR 2100. **C.** Illustration of landmark positions used for articulated skull. Black circles, landmarks; white circles interconnected with solid lines, semilandmarks. **D.** Ontogenetic shape change visualized by deformation grids for 2D data (see Bhullar et al. 2012).

Fig. 2. Landmarks and semilandmarks designated using tpsDIG for 2D data (A) and LANDMARK for 3D data (B). Landmark configurations aligned using generalized procrustes analysis, removing the effects of size, orientation, and position (C, D). Ontogenetic shape change visualized by generating deformation grids for 2D data (E) and warped meshes for 3D data (F).

Fig. 3. Representative premaxillae (rendered CT images) of *Majungasaurus crenatissimus* (Depéret, 1896) Lavocat, 1955 from the Maastrichtian (Late Cretaceous) Maevarano Formation, northwestern Madagascar in right lateral view. **A.** FMNH PR 3369. **B.** FMNH PR 2278. **C.** Illustration of landmark positions used for premaxillae. Black circles, landmarks; white circles interconnected with solid lines, semilandmarks. **D.** Ontogenetic shape change visualized by deformation grids relative to average; outline of smallest (D<sub>1</sub>) and largest (D<sub>2</sub>) specimens from average.

Fig. 4. Representative maxillae (rendered CT images) of *Majungasaurus crenatissimus* (Depéret, 1896) Lavocat, 1955 from the Maastrichtian (Late Cretaceous) Maevarano Formation, northwestern Madagascar in right lateral view. **A.** UA 9944. **B.** FMNH PR. 3369. **C.** FMNH PR 2278. **D.** Illustration of landmark positions used for maxillae. Black circles, landmarks. **E.** Ontogenetic shape change visualized by deformation grids relative to average; outline of smallest (E<sub>1</sub>) and largest (E<sub>2</sub>) specimens from average.

Fig. 5. Representative lacrimals (rendered CT images) of *Majungasaurus crenatissimus* (Depéret, 1896) Lavocat, 1955 from the Maastrichtian (Late Cretaceous) Maevarano Formation, northwestern Madagascar in left lateral view. **A.** UA 9944. **B.** FMNH PR 2100. **C.** Illustration of landmark positions used for lacrimals. Black circles, landmarks; white circles interconnected with solid lines, semilandmarks. **D.** Ontogenetic shape change visualized by deformation grids relative to average; outline of smallest (D<sub>1</sub>) and largest (D<sub>2</sub>) specimens from average.

Fig. 6. Representative postorbitals (rendered CT images) of *Majungasaurus crenatissimus* (Depéret, 1896) Lavocat, 1955 from the Maastrichtian (Late Cretaceous) Maevarano Formation, northwestern Madagascar in right lateral view. **A.** UA 9944. **B.** FMNH PR 3369. **C.** FMNH PR 2100. **D.** Illustration of landmark positions used for postorbitals. Black circles, landmarks; white circles interconnected with solid lines, semilandmarks. **E.** Ontogenetic shape change visualized

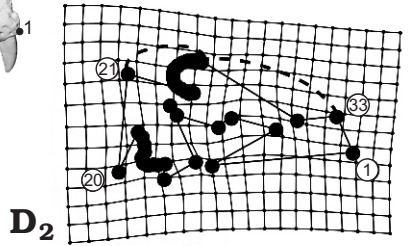
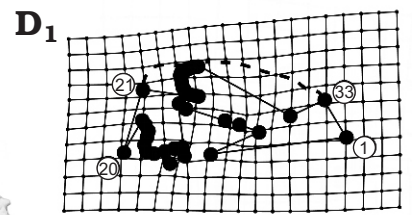
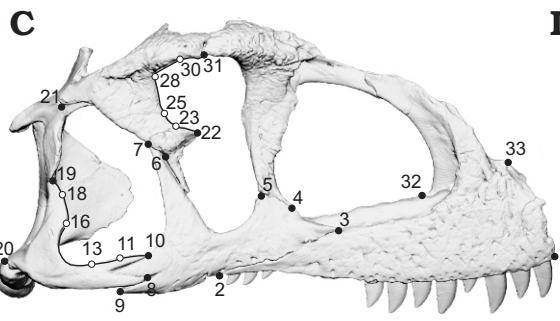
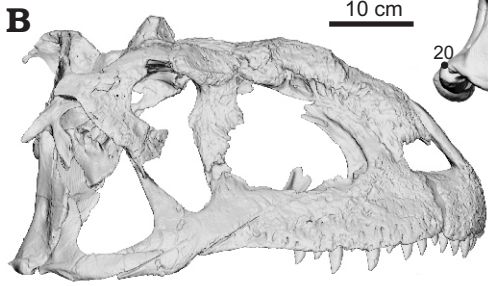
by deformation grids relative to average; outline of smallest ( $E_1$ ) and largest ( $E_2$ ) specimens from average.

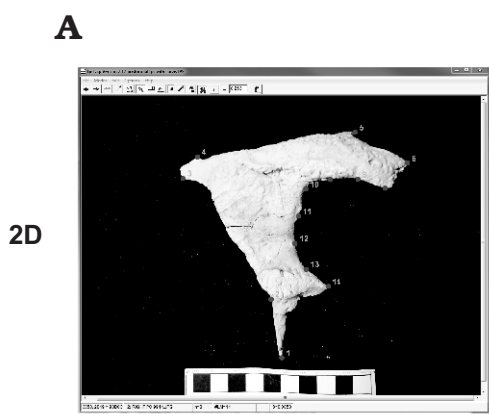
Fig. 7. Representative jugals (rendered CT images) of *Majungasaurus crenatissimus* (Depéret, 1896) Lavocat, 1955 from the Maastrichtian (Late Cretaceous) Maevarano Formation, northwestern Madagascar in right lateral view. **A.** UA 9944. **B.** FMNH PR 3369. **C.** FMNH PR 2100. **D.** Illustration of landmark positions used for jugals. Black circles, landmarks. **E.** Ontogenetic shape change visualized by deformation grids relative to average; outline of smallest ( $E_1$ ) and largest ( $E_2$ ) specimens from average.

Fig. 8. Representative right quadrates (rendered CT images) of *Majungasaurus crenatissimus* (Depéret, 1896) Lavocat, 1955 from the Maastrichtian (Late Cretaceous) Maevarano Formation, northwestern Madagascar in left lateral view. **A.** UA 10000. **B.** UA 9944. **C.** FMNH PR 3369. **D–F.** Landmark positions in anterior (D), left lateral (E), and posterior (F) views. **G, H.** Warped meshes, rostral (G) and lateral (H) views, showing idealized transformation of smallest (s) to largest (l) elements in the size range examined.

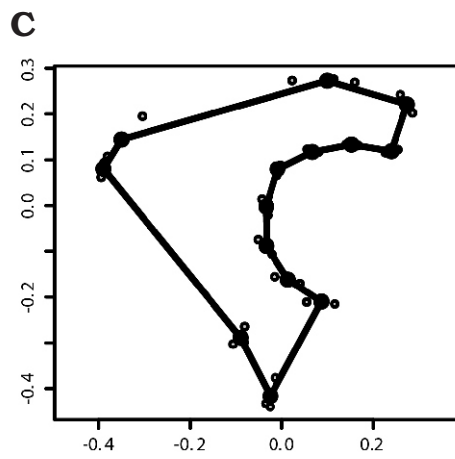
Fig. 9. Representative dentaries (rendered CT images) of *Majungasaurus crenatissimus* (Depéret, 1896) Lavocat, 1955 from the Maastrichtian (Late Cretaceous) Maevarano Formation, northwestern Madagascar in left lateral view. **A.** MAD 10440. **B.** FMNH PR 2100. **C.** Illustration of landmark positions used for dentaries. Black circles, landmarks; white circles interconnected with solid lines, semilandmarks. **D.** Ontogenetic shape change visualized by deformation grids relative to average; outline of smallest ( $D_1$ ) and largest ( $D_2$ ) specimens from average.

Fig. 10. Representative surangulars (rendered CT images) of *Majungasaurus crenatissimus* (Depéret, 1896) Lavocat, 1955 from the Maastrichtian (Late Cretaceous) Maevarano Formation, northwestern Madagascar in left lateral view. **A.** FMNH PR 3369. **B.** FMNH PR 2100. **C.** Illustration of landmark positions used for surangulars, UA 9944 (not to scale). Black circles, landmarks; white circles interconnected with solid lines, semilandmarks. **D.** Ontogenetic shape change visualized by deformation grids relative to average; outline of smallest ( $D_1$ ) and largest ( $D_2$ ) specimens from average.

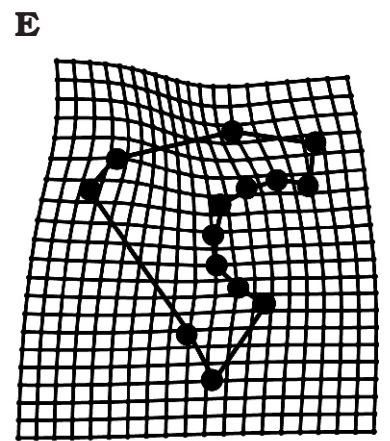




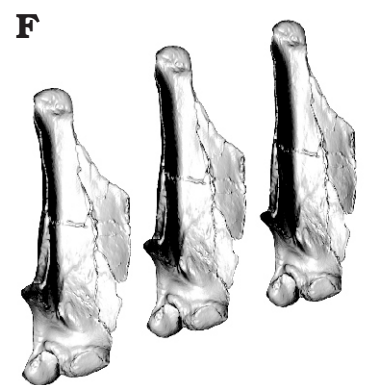
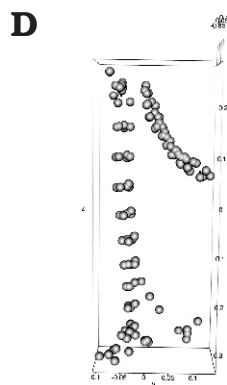
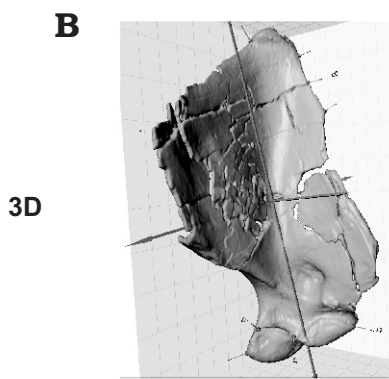
designate landmarks

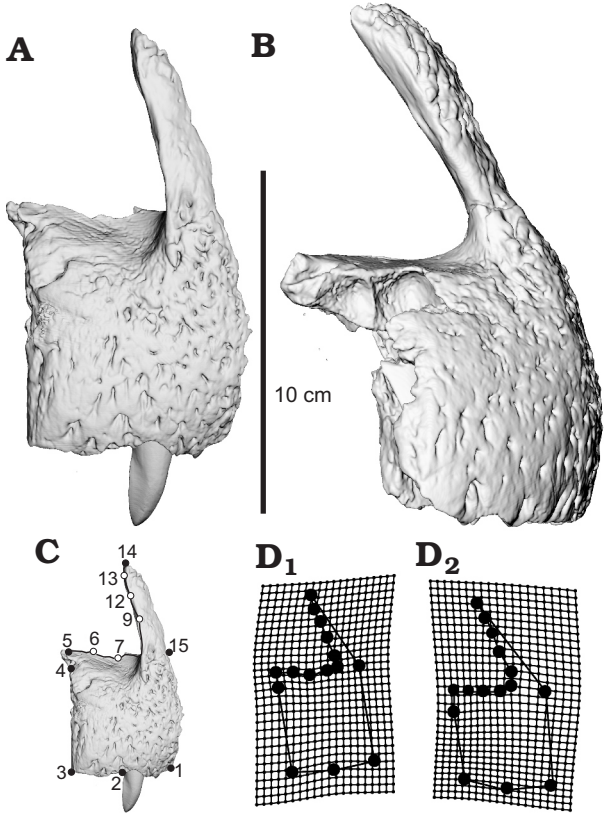


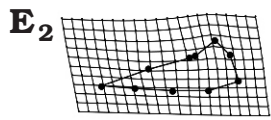
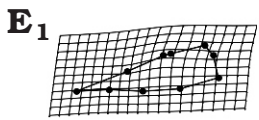
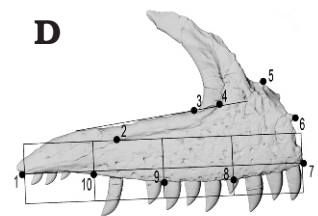
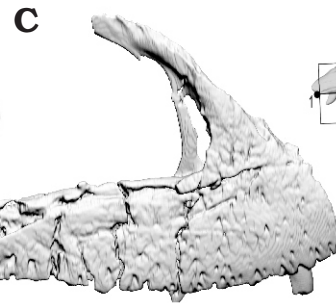
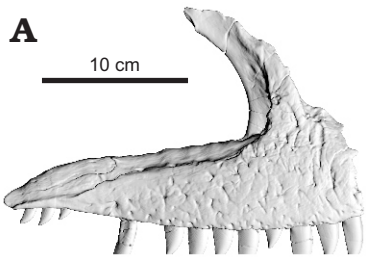
apply generalizes procrustes analysis

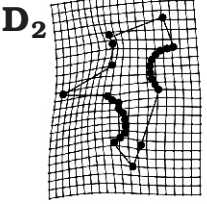
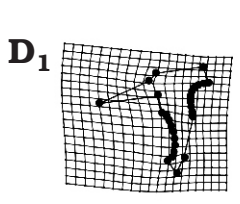
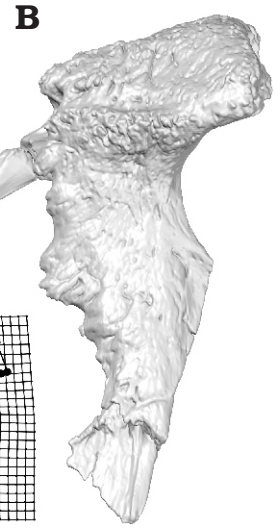
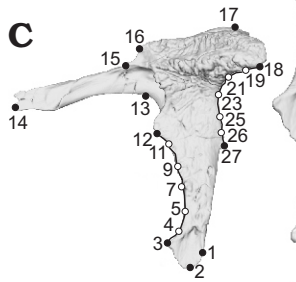
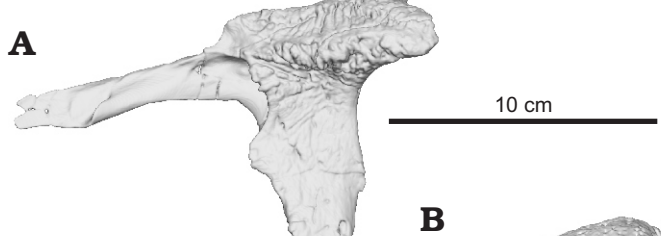


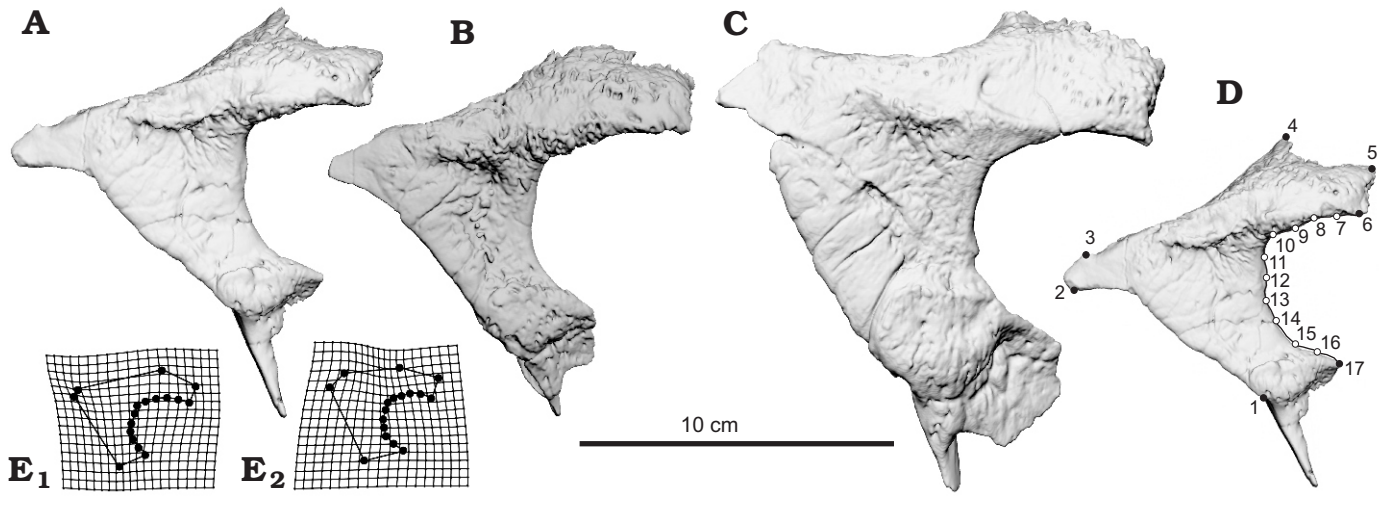
generate shape change visualizations



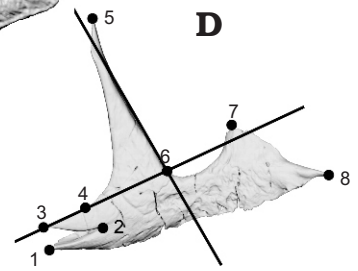
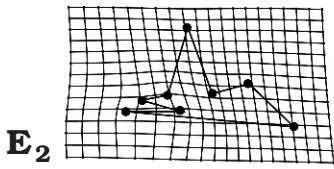
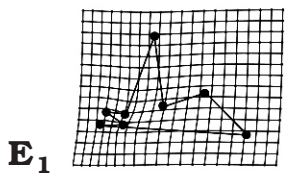
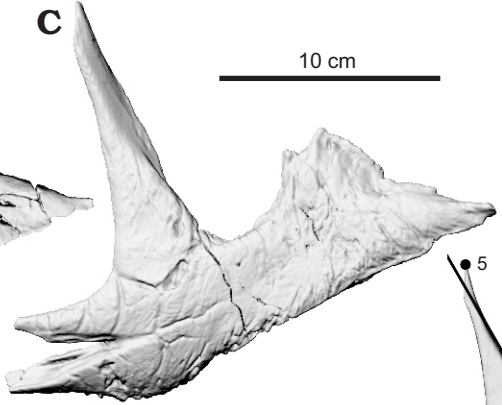
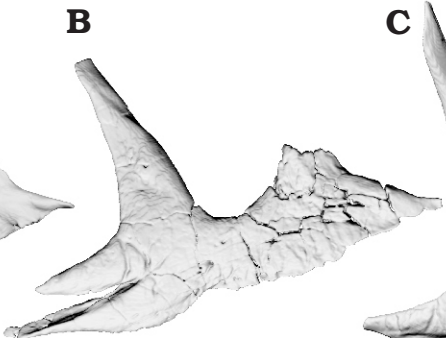
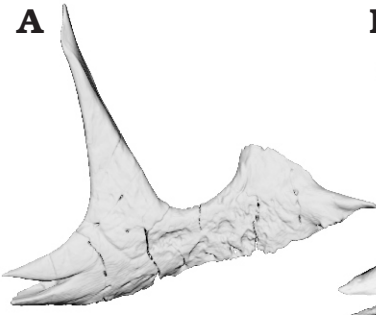


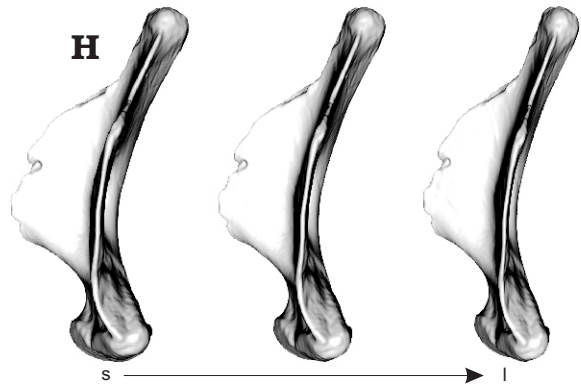
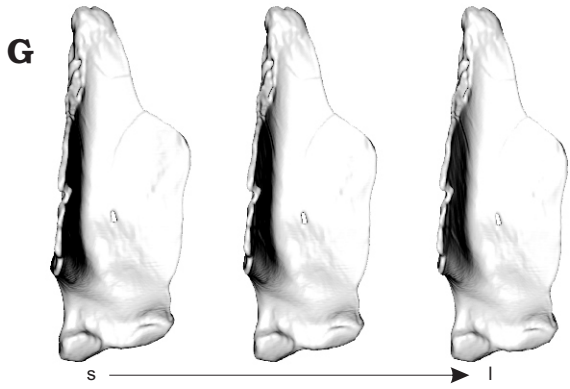
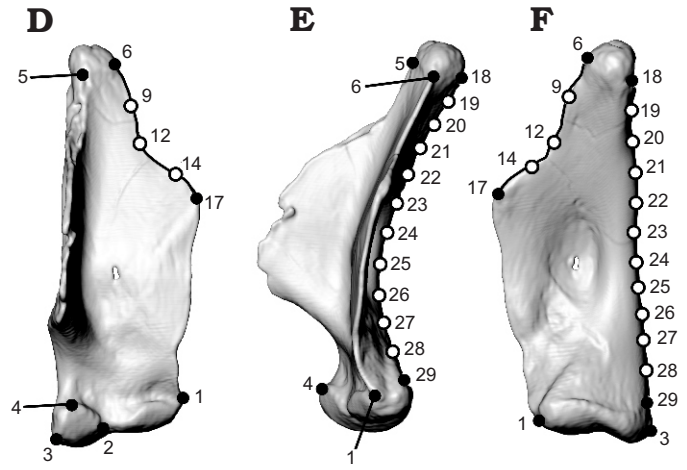
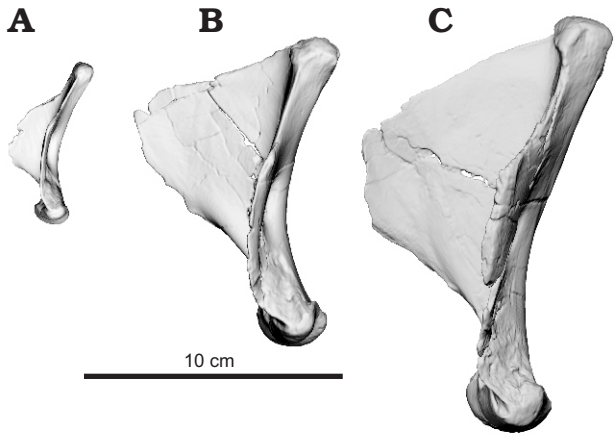


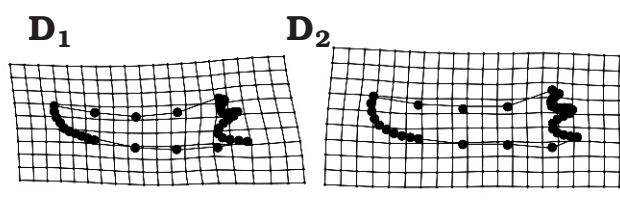
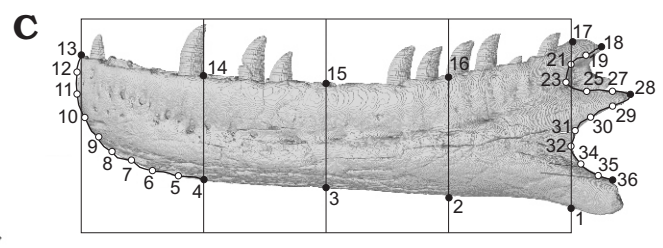
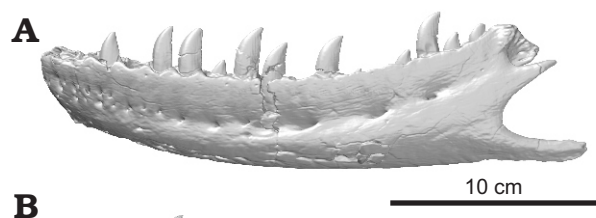












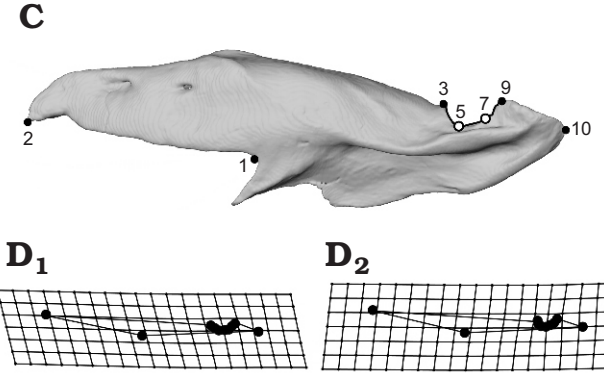
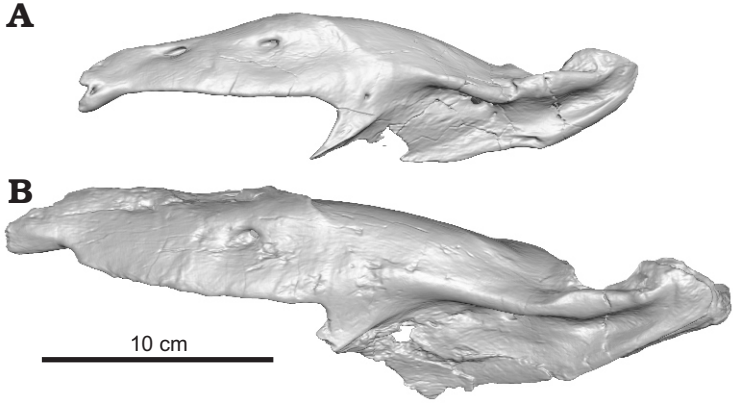


Table 1. List of isolated elements of *Majungasaurus crenatissimus* used in this study.

| Specimen  | Element     | Number of specimens | Number of landmarks | Number of semilandmarks |
|---|-------------|---------------------|---------------------|-------------------------|
| FMNH PR 2278, FMNH PR 3369, UA 8716, UA 8717, UA 9944       | Premaxilla  | 5                   | 7                   | 8                       |
| FMNH PR 2100, FMNH PR 2278, FMNH PR 3369, UA 9944,          | Maxilla     | 4                   | 7                   | 3                       |
| FMNH PR 2100, UA 9944                                       | Lacrima     | 2                   | 11                  | 16                      |
| FMNH PR 2100, FMNH PR 3369, UA 9944                         | Postorbital | 3                   | 7                   | 10                      |
| FMNH PR 2100, FMNH PR 3399, UA 9944                         | Jugal       | 3                   | 6                   | 2                       |
| FMNH PR 2100, FMNH PR 2278, FMNH PR 3369, UA 9944, UA 10000 | Quadrate    | 5                   | 9                   | 16                      |
| FMNH PR 2100, FMNH PR 3369, UA 9944                         | Dentary     | 3                   | 12                  | 24                      |
| FRMNH PR 2100, FMNH PR 3369, UA 9944                        | Surangular  | 3                   | 5                   | 5                       |

Table 2. List of *Majungasaurus crenatissimus* skull specimens used in this study.

| Accession number | Locality  | Skull elements preserved  |
|------------------|-----------|---|
| FMNH PR 2100     | MAD 96-01 | Nearly complete, exquisitely preserved, disarticulated skull (see Sampson and Witmer 2007 for complete list of elements)  |
| FMNH PR 2278     | MAD 99-26 | Associated cranial material (both: premaxillae, maxillae; left: jugal, quadratojugal, ectopterygoid, quadrate, surangular, angular, prearticular, articular)            |
| FMNH PR 3369     | MAD 05-42 | Right: maxilla, postorbital, surangular, quadrate (note: additional elements are preserved, but not yet prepared)   |
| UA 9944          | MAD 05-42 | Left: dentary, premaxilla; both: postorbitals, jugals, splenials, ectopterygoids, lacrimals, quadrates, surangulars, angulars; right: maxilla, squamosal, quadratojugal |
| UA 10000         | MAD 05-42 | Basisphenoid; left: maxilla, jugal, quadrate  |